Criticality configuration design methodology applied to the design of fuel debris experiment in the new STACY

Satoshi Gunji, Kotaro Tonoike, Jean Baptiste Clavel, Isabelle Duhamel

ARTICLE

Criticality configuration design methodology applied to the design of fuel debris experiment in the new STACY

Satoshi Gunji[a*] Kotaro Tonoike[a], Jean-Baptiste Clavel[b] and Isabelle Duhamel[b]

[a] *Japan Atomic Energy Agency, 2-4 Shirane, Shirakata, Tokai-mura, Naka-gun, Ibaraki 319-1195, Japan ;*

[b] *Institut de Radioprotection et de Sûreté Nucléaire (IRSN), Fontenay-aux-Roses, 92260, France*

The new critical assembly STACY will be able to contribute to the validation of criticality calculations related to the fuel debris from Fukushima Daiichi Nuclear Power Plant. The experimental core designs are in progress in the frame of JAEA/IRSN collaboration. This paper presents the method applied to optimize the design of the new STACY core to measure the criticality characteristics of pseudo fuel debris that simulated Molten Core Concrete Interaction (MCCI) of the fuel debris. To ensure that a core configuration is relevant for code validation, it is important to evaluate the reactivity worth of the main isotopes of interest and their k_{eff} sensitivity to their cross sections. In the case of the fuel debris described in this study, especially for the concrete composition, silicon is the nucleus with the highest k_{eff} sensitivity to the cross section. For this purpose, some parameters of the core configuration, as for example the lattice pitches or the core dimensions, were adjusted using optimization algorithm to find efficiently the optimal core configurations to obtain high sensitivity of silicon capture cross section. Based on these results, realistic series of experiments for fuel debris in the new STACY could be defined to obtain an interesting feedback for the MCCI. This methodology is useful to design other experimental conditions of the new STACY.

*Corresponding author. Email: gunji.satoshi74@jaea.go.jp

Keywords: Fukushima Daiichi Nuclear Power Plant; critical experiment; fuel debris; MCCI; new STACY; sensitivity analysis, experimental design, optimization method

1. Introduction

The Japan Atomic Energy Agency (JAEA) intends to re-start the Static Experiment Critical Facility (STACY) [1] to perform experiments in support of post-Fukushima safety activities. The objective of the intended research using the new STACY critical facility is to establish an improved database for criticality safety. In particular, this database is expected to assist in the removal of fuel debris from the Fukushima Daiichi Nuclear Power Plant. Indeed, in the validation of criticality safety codes using data bases such as the ICSBEP [2], there is no experimental data representative of the molten-core-concrete-interaction (MCCI).

The new STACY is a light water moderated critical assembly with lattice of UO_2 rods in the water tank. It will be able to use pseudo fuel debris, which is sample rods composed of UO_2 powder mixed with materials included in fuel debris. The ^{235}U enrichment of the 900 UO_2 rods, which have been recently manufactured and the UO_2 powder to make the specific sample rods, are the same and slightly less than 5 wt.%. **Table 1** shows some specifications of the new STACY.

Some specific sample rods will be manufactured to simulate one important characteristic of "fuel debris", the molten-core-concrete-interaction that mixed UO_2 with concrete. For this purpose, a small fabrication facility will be constructed in order to manufacture pseudo fuel debris samples using uranium oxide, iron, zircaloy, concrete, and other materials included inside/outside of commercial reactor vessels.

This paper estimates the potential of the criticality experimental design, for the concrete validation, using mixt pseudo fuel debris and full concrete rods. In addition, this paper shows the methodologies to define experimental core configurations of the new STACY for the measurement of the criticality characteristics. This method is based on the optimization approach on the effective multiplication factor (k_{eff}) sensitivity to the cross section and the studies of the sensitivity energy profiles and neutron spectra in the core.

2. Sensitivity analysis

The experimental results related to the study of the MCCI condition will be a unique source of information not yet available in the literature. . Criticality of the MCCI type fuel debris depend on various characteristics such as the concrete compositions the moderation ratio, fuel debris size and mass. It is important to note that these composition and moderation ratio are very uncertain. For the work presented in this paper, the concrete composition used is shown in **Table 2** [3]. This composition was used in previous studies, but it does not necessarily represent the MCCI in the Fukushima Daiichi accident. Similarly, the fissile material under consideration is uranium enriched to 5%, which does not correspond to a composition derived from Fukushima accident but is representative to the reactor fresh fuel. In general, there are various compositions of concrete-fuel mixture in the Fukushima Daiichi accident. Therefore, it will be necessary to analyze various compositions, evaluate the dispersion of the compositions, and validate the representative results by critical experiments.

Before starting the design of the experiments, one should define the application cases of interest to have one target that will be compared with the experimental design results. **Figure 1** shows one of the application cases considered in criticality safety studies. It consists of a lattice of fuel debris surrounded by light water. The spheres (r = 1cm) of the MCCI type fuel debris are composed of UO_2 (5 wt.% enriched ^{235}U) mixed with the concrete with concrete volume fractions equal to 0.2 and 0.6. The concrete volume fraction (CVF) is defined by the following equation:

$$CVF = \frac{V_C}{V_{UO_2+V_C}} \quad (1)$$

where V_C and V_{UO_2} are volumes of the concrete and UO_2, respectively.

Moderation ratio is one of the most important parameters for evaluating criticality characteristics, because it has an impact on the neutron spectra. Moderator-to-fuel volume ratio is defined by Equation (2). Experimentally, it will be able to change lightly this value by adjusting the lattice pitches (interval between rods).

$$\frac{V_m}{V_f} = \frac{Volume\ of\ the\ moderator\ (H_2O)}{Volume\ of\ the\ fuel\ (UO_2)} \quad (2)$$

For the application case, the spheres are located in a face-centered cubic (FCC) lattice. The interval between these spheres is adjusted to obtain arbitrary V_m/V_f values, and the effective diameter of the debris spheres lattice is adjusted to obtain the k_{eff} value equal to 1.

The k_{eff} sensitivity (S) to the cross section (σ) is the relative effect on the k_{eff} caused by a perturbation of the cross section of the reaction i of the nucleus j.

$$S_{ij} = \frac{\partial k \cdot \sigma_{ij}}{k \cdot \partial \sigma_{ij}} \quad (3)$$

These calculations are used to estimate the influence of an isotope on the k_{eff} and more precisely, the reactions and energy domains having an impact on the k_{eff} value. If the sensitivity to a cross section of an isotope is high, this means that it has a significant weight on the reactivity of the studied configuration and that it is potentially feasible to provide relevant feedback on nuclear data assessments.

These sensitivity analyses for the application cases were calculated with MCNP6.1 [4] code using JENDL-4.0 [5] library. The sensitivities of all reaction for all nuclides were calculated using "KSEN" option of MCNP6.1 in 238 neutron energy groups. From previous study [3], it is known that k_{inf} of the MCCI type fuel debris varies greatly depending on the values of V_m/V_f. In each CVF, the values of k_{inf} become maximum at around $V_m/V_f = 1$. Therefore, $V_m/V_f = 1$ was selected in this application cases.

The analyses of the k_{eff} sensitivities to the cross sections of the application case are performed. It shows that there is no significant change in the energy profiles of the sensitivity to the fissile nuclei reactions and on their magnitudes, such as ^{235}U fission and ^{238}U capture. So it is not considered as an optimization target in the process of core configuration design. The energy profiles of these sensitivities obtained for the new STACY final design were compared with those of the application cases (only MCCI debris). It confirmed that there is no significant difference.

The k_{eff} sensitivities to the cross sections of the nuclei that composed the concrete were studied to define the optimization target for the experimental design investigation. **Table 3** shows the results obtain for two critical ($k_{eff} = 1$) configurations of the application case with CVF = 0.2 and CVF = 0.6. Eight reactions with large k_{eff} sensitivities among the components derived from the concrete are shown in Table 3. The capture reactions were selected as the reaction of interest in this study since, when CVF is changed from 0.2 to 0.6, the absolute integral value of the capture reaction of ^{28}Si, ^{40}Ca, ^{39}K, ^{56}Fe, ^{27}Al, and the contribution rates among the integral sensitivities of these concrete-derived nuclei change.

The energy profiles of the sensitivities to capture cross sections for the main concrete isotopes at CVF = 0.2 and CVF = 0.6 cases are shown in **Figure 2**. One observers that an increase on the CVF values from 0.2 to 0.6, leads to an increase on the sensitivity integral value for all nuclei. In particular, the contribution of the sensitivity peak in thermal energy increases. This is because high CVF means more concrete amount and so more reaction probability for the concrete nuclei. Additionally, the concrete contributes to neutron moderation (such as because hydrogen contain in the concrete is not take into account in the V_m/V_f calculation). Another observations are that ^{28}Si, ^{39}K, ^{56}Fe, ^{23}Na, and ^{27}Al have similar profile shapes while the profile shape of ^{40}Ca is different as can be clearly seen in the fast energy region.

Based on these results, the k_{eff} sensitivity to the ^{28}Si capture reaction (S_^{28}Si) was selected as the optimization target to the core configuration design prospection. To account for the ^{40}Ca, the value and energy profiles of the k_{eff} sensitivity to the capture (S_^{40}Ca) was checked for the configurations selected by the design optimization method.

3. Core configuration design

3.1. Experimental constraints and choices

The new STACY will have several experimental constraints due to its design

limitation and its operating authorization. Only some constraints of the new STACY were considered in this study, which are shown in **Table 4**. As for the number of fuel rods, 900 new fuel rods will be able to be used in future designs, but only 400 old fuel rods already available were used in this study. Moreover, samples composed with only concrete and a zircaloy cladding identical to the fuel rod were used for the work presented in this paper, taking into account that previous results [6] have showed that the characteristics of the MCCI type fuel debris can be measured using 100 % concrete samples. In addition, it is simplest and less expensive to use in the critical experiments full concrete rod than the mixt (UO_2 and concrete) pseudo fuel debris samples.

The water height of the new STACY that will be able to maintain critical state must be comprised between 40 and 140 cm, but it is known that the uncertainty will increase if is the water level is not up to 110 cm [1]. Therefore, in this study, optimizations were performed with a fixed critical water height of 130 cm.

In the new STACY, the reactivity worth of loaded samples will be evaluated by measuring differences of the water height with and without samples. For each experiment two configurations are carried out: one with the studied samples and one without this sample (the sample is usually substituted by void tubes). From these two results, the reactivity worth (ρ_{exp}) is measured by following the equation, based on one-group diffusion theory.

$$\rho_{exp} = \frac{A}{2} \times \left\{ \frac{1}{(H_1 + \lambda)^2} - \frac{1}{(H_0 + \lambda)^2} \right\} \quad (4)$$

where, A is the constant, λ is the extrapolation length. H_1 is the critical water height with pseudo fuel debris samples, and H_0 is the experiment without samples. It is desirable that the reactivity is in between 10 to 500 pcm, by considering the uncertainty of the water level gauge and changes in buckling.

3.2. Optimization Method and Tools

The goal of the core configuration optimization was to maximize S_^{28}Si. In order to

do that, many batches of calculations were performed with the MCNP6.1 code and JENDL-4.0 library processed by NJOY99. The optimizations were managed by the IRSN PROMETHEE workbench [7] and EC-EGO (Equality Constraint Efficient Global Optimization) algorithm [8]. Several optimizations were performed with various input parameters as for examples, the lattice pitch or CVF in the fuel debris sample rods. This approach allows exploring a large space of possibilities by limiting the number of calculations.

By using these methods, a previous study [6] was performed for an "ideal" cylindrical core arrangement without constraints. For this case core was only constituted by rods composed with a mixt of UO_2 and concrete. This mixt is meant to simulate the fuel debris. A configuration optimization was performed to estimate the k_{eff} sensitivities to the Si capture cross-section ($S\_^{28}Si$) that could be expected and $S\_^{40}Ca$ was also calculated. The sensitivity results were around $-2.18 \cdot 10^{-2}$ and $-5.79 \cdot 10^{-3}$, respectively for $S\_^{28}Si$ and $S\_^{40}Ca$. Hence, the experimental design configuration study presented in this present paper approach to the "ideal" cylindrical core results.

During the optimization calculations presented in this paper, the configuration type is a square lattice arrangement of the fuel rods and the concrete rods. It is made automatically with a simple R-function developed for this purpose [6]. The goal of this function is to obtain a uniform distribution of the pseudo fuel debris rods in the square lattice. However, the arrangements obtained with this method are not regular in the sense that the reproducibility of the experimental set-up is not easy achieved. Therefore, an adjustment is made to have simplest configurations with equivalents number of samples after this optimization.

3.3. Original two-zones core configurations

Among the types of configurations studied, two-zones core configurations were considered in order to take into account the restriction on the upper limit of the fuel rods

number. As shown in **Figure 3**, different pitch sizes of each zone were defined as optimization parameters. An "Experimental zone", where the concrete sample rods are inserted, is located in the center of the core. The external zone is a "Driver zone" made only of fuel rods to achieve criticality.

Other parameters used for the configuration optimization are shown in **Table 5**. Among them, the loading ratio of the sample (w) is defined by Equation 4, where N_f and N_c are respectively the number of fuel rods in the experimental zone (UO_2 fuel rods in the driver zone are not taken into account) and the number of the concrete rods in the experimental zone.

$$w = \frac{N_c}{N_c + N_f} \quad (5)$$

The optimization goal is to obtain the maximum absolute values of $S_{-}^{28}Si$. The algorithm also takes into account the constraint to have a multiplication factor slightly larger than 1 (~1.001). The MCNP calculations for the optimization were computed using 1,000 histories per generation with 300 active generations after 50 inactive generations (the magnitudes of the calculation uncertainties are $1\sigma(k_{eff}) < 160$ pcm, $1\sigma(S_{-}^{28}Si)$ around 3.5 %). These calculation accuracies are acceptable for the optimization phase that requires a high number of calculations and therefore require a compromise between precision and calculation times.

At the end of the optimization process, all the calculation results are analyzed. **Figure 4** shows the distribution of calculations in the parameters space and the results as a function of each parameter. Each point represents the projection per pair of the calculation parameters values and the results. With this graph, the correlation between optimization parameters, k_{eff}, and $S_{-}^{28}Si$ can be studied. First of all, combinations of parameters that give results with k_{eff} larger than 1 are selected. It is obvious that $S_{-}^{28}Si$ is correlated with the loading ratio of the sample w. In order to obtain higher value of $S_{-}^{28}Si$, the smaller pitches of the experimental zone P1 and the larger sizes of the experimental zone D1 are privileged. This allows loading more concrete sample rods. On the other hand, the pitch of the driver zone P2

and the size of the driver zone D2 show no tendencies. Therefore, P2 and D2 are of lesser importance in this optimization process.

The optimization approach automatically generates the configuration with the parameter values proposed by the algorithm. In this way, D1 was determined by the algorithm and the proposed value was automatically adjusted to be an odd integer multiple of P1. However, the connection between the two regions was not taken into account and P2 is not linked to D1 and D2.Consequently, D2 was not set to be an odd integer multiple of P2 and the boundary of the external core can lead to incomplete fuel cells. Therefore, in some cases, fuel element cells were cut, and the obtained unrealistic shapes were simulated (see **Figure 5**).

To obtain more realistic configurations, those selected by the optimization process had to be modified manually. For that, the incomplete fuel cells between the two regions were replaced with water gaps, and the outside of the driver zone was replaced with cells having the correct fuel rod shape. During the configuration changing, the number of fuel rods in the peripheral zone was adjusted to conserve an equivalent k_{eff}. At the end of this configuration adjustment, the $S\_^{28}Si$ did not changed significantly compared to the unrealistic optimized configuration.

As results of the optimization process, three basic core configurations with different values of V_m/V_f and different sizes of the experimental zone were defined, namely, different P1 and D1 were selected to make different condition of V_m/V_f in the experimental zone for which details are shown in **Table 6** and **Figure 6**. Each configuration is assigned an ID derived from the sizes of the experimental zone, like T25, T21, and T15. The size of each experimental zones is almost the same and close to the D1 maximum value (25 cm). The configuration T25 has the smaller pitch of the experimental zone, so it has larger concrete rods number. On the other hand, the configuration T15 has the larger pitch and the lower number of concrete sample rods.

3.4. Neutron energy spectra in the experimental zones

The neutron energy spectra variation in the experimental zones was investigated for the selected configurations. As described above, the pitches in the two zones and for each configuration are different. In addition, the water gaps between the two zones are also different. By consequence, the neutron energy spectrum may be heterogeneous in the experimental zone. As the k_{eff} sensitivity of the capture reactions are energy dependent, it is important to verify that all the concrete samples have a similar contribution to the k_{eff} sensitivity. Thus, the neutron energy spectra in the experimental zone must be as homogeneous as possible.

For the three configurations, the neutron energy spectra of each experimental zone were divided in three areas to compare the neutron spectrum depending of the sample position. For that, three areas were named, "center", "middle", and "outer edge," respectively. **Figure 7** shows normalized and cell averaged neutron flux densities in each experimental zone. At first, in the case of T21, the neutron energy spectra from "center" to "outer edge" are in good agreement, so it shows there is no significant difference in the three areas. On the other hand, in the cases of T25 and T15, it is found that there is small difference in the thermal peaks. In other words, the neutron energy spectra in the experimental zones vary slightly from place to place, and this can affect also the k_{eff} sensitivities. It is necessary to investigate the integral sensitivities of each area for each energy.

3.5. Comparative study of sensitivity depending on sample loading positions

The k_{eff} sensitivities at each area were compared to evaluate the effects of the neutron energy spectra difference in function of the position. The $S\_^{28}Si$ and $S\_^{40}Ca$ normalized by the number of samples in each area were compared for three energy groups. **Table 7** shows the results. The maximum sensitivities difference is in the thermal neutron energy group for the $S\_^{40}Ca$ in the T21 case. But the difference of magnitude is at most of 1.5% between the

"center" and the "outer edge." Since the T21 core configuration has the most homogeneous neutron energy spectrum in the experimental zone among the three selected core configurations, it is considered that the slight heterogeneity of the neutron energy spectrum was not significant for the experimental objective.

From these results, the interests of the two-zones core configurations were confirmed.

3.6. Making realistic core configurations

Three core configurations with different pitches and sizes of the experimental zone were selected, but the loading patterns in this zone are too complicated to be realized by the operators. In fact, they were automatically generated by the R-function based on random approached using the Latin Hypercube Sampling method, with the goal to obtain a uniform distribution of the concrete samples. So, the patterns produced are not symmetric and easy to reproduce. Consequently, it is desirable for making experimental core configurations to have simple arrangement of the concrete rods. For this purpose, an adjustment of the internal core was performed to have regular patterns to keep the same number of concrete rods. After that, it is important to check the values of the integral sensitivity to evaluate the impact of the pattern modification.

In addition to verifying the efficiency of the optimization method, several regular insertion patterns in the experimental zones were studied for each core configuration for different number of concrete rods. The reactivity worth was estimated, for each case, by replacing the concrete sample rods with Zircaloy void tubes and evaluating the critical water heights. The MCNP calculations for this series were computed using 5,000 histories per generation with 1,000 active generations after 100 inactive generations (the magnitudes of the calculation uncertainties are $1\sigma(k_{eff})$ 30 pcm, $1\sigma(S\_^{28}Si)$ around 0.5 %).

Figure 8 shows the results of sensitivities ($S\_^{28}Si$ and $S\_^{40}Ca$) and reactivity worth for the configurations from the optimization method, with the regular patterns and for different

concrete rods. The open marks are the original loading patterns generated by the R function, and the filled marks are the regular patterns. The first observation is that there is no significant impact of the arrangement modification on the S_^{28}Si, S_^{40}Ca and the reactivity worth. Indeed, if we compare the results from similar configuration with the same (or close) number of concrete rods, the difference is negligible.

Moreover, the absolute values of the integral sensitivity became maximum for the number of concrete rods close to the number predicted by the optimization. So, this method seems an interesting way to investigate and design experiments. As the results, 544 (T25), 372 (T21), and 140 (T15) rods patterns were selected.

Figure 8 also shows that as the number of samples increased, the reactivity worth tends to increase up to a threshold for a high number of concrete rods. The sign change of the reactivity worth highlights the complexity of the concrete impact that is not only due to the capture effect but also the addition of different effects. It should be noted that for the configuration close to the best S_^{28}Si, the reactivity worth is relatively small. In addition, the difference of water height between the configurations with concrete rods and with void tubes is measurable (< 500 pcm). These observations are interesting for the experimental conditions and the associated safety constraint.

The final core configurations were selected as results of this study. They are shown in **Figure 9** and their specifications in **Table 8**. For each core, one can expect integral sensitivities of 41 %, 35 %, and 15 % relative to the sensitivity obtained for an "ideal" cylindrical configuration discussed at the end of Section 2. However, the values of the sensitivity per sample rod were larger in the two-zone configurations than the ideal case. This can be explained by the fact that the optimization had considered only full concrete rods (CVF = 1) whereas the ideal case was composed of mixt pseudo fuel debris (CVF < 1). So, in this cylindrical configuration, the samples have a less quantity of concrete. They are composed by a mixt of UO_2 and concrete probably more closed to the "real" fuel debris.

The consequence of the smaller quantity of concrete per rod is a lower $S\_^{28}Si$ per rod.

The comparisons of the energy profiles of $S\_^{28}Si$ and $S\_^{40}Ca$ show that the shapes do not change significantly between the three core configurations and the ideal case.

Among these core configurations, the T25 core configuration with its large number of sample rods conducts to the highest $S\_^{28}Si$. On the other hand, the highest sensitivity per sample corresponds to the T15 core configuration.

These three configurations of two-zone core satisfy the experimental and regulator constraints, therefore they are conceivable in the new STACY. Furthermore, the core configuration optimization method in this study is efficient, so it will be used effectively for future STACY experiments that includes the measurement of the criticality characteristics of various fuel debris.

4. Conclusion

New STACY's experimental core configurations were studied to measure the critical characteristics of MCCI type fuel debris by criticality experiments. In this study, the k_{eff} sensitivity to the ^{28}Si capture reaction is the important indicator to drive the design process. The second interesting nucleus is the ^{40}Ca, because the profile of k_{eff} sensitivity to the ^{40}Ca capture cross section is slightly different.

The method used to define the best core configuration to have an interesting feedback on the critical concrete characteristics is based on the EC-EGO algorithm. This optimization was performed using PROMETHEE workbench and an R-function to define automatically a uniform concrete rod arrangement.

The target of the optimization was to maximize the integral value of the capture sensitivity of ^{28}Si ($S\_^{28}Si$) in the experimental two-zones core configurations. The pitches and sizes of experimental and driver zones were defined as parameter for the optimization. The other parameter was proportion of concrete rods in the experimental zone. The results of these

optimization showed that the size of the experimental zone is always the maximal value of the variation range define for this parameter. Three core configurations with different pitches were selected for the next part of the study.

The configurations generated by the algorithm had required some adjustment to be more realistic and less complicated to be applied in real experimental conditions. The comparisons of the neutron energy spectra in each experimental zone showed that the impact of the modification is not significant as well as the effect to the energy profiles of the k_{eff} sensitivities to the ^{28}Si and ^{40}Ca capture reactions. It is also confirmed that the configuration generated by the optimization process obtained the optimum value of the S_^{28}Si.

The reactivity worth was also evaluated. For the better configuration in term of S_^{28}Si, the magnitude of the reactivity worth and variation range of the water height between the configuration with concrete rods and with void tube satisfied the experimental constraints of the new STACY.

Critical experiments using the new STACY will be able to contribute to retrieval works of Fukushima Daiichi Nuclear Power Plant. In this study, optimal experimental core configurations were presented especially when the larger sensitivity of Si in MCCI was needed. To simulate real reactor conditions, it is necessary to reconfirm the core conditions of the new STACY by using the latest knowledge such as fuel debris sampling results of the fuel debris and concrete composition information.

Acknowledgements

Work reported in this paper was performed under the auspices of Secretariat of Nuclear Regulation Authority (S/NRA/R) of Japan.

References

[1] Izawa K., Tonoike K., Leclaire N., Duhamel I. DESIGN OF WATER-MODERATED

HETEROGENEOUS CORE IN NEW STACY FACILITY THROUGH JAEA/IRSN COLLABORATION. Proceedings of ICNC2015; 2015 Sep. 13-17; Charlotte, USA. [CD-ROM].

[2] International Handbook of Evaluated Criticality Safety Benchmark Experiments, July 2019, OECD/NEA

[3] Tonoike K., Ohkubo K., Takada T. CRITICALITY CHARACTERISTICS OF MCCI PRODUCTS POSSIBLY PRODUCED IN REACTORS OF FUKUSHIMA DAIICHI NUCLEAR POWER STATION. Proceedings of ICNC2015; 2015 Sep. 13-17; Charlotte, USA. [CD-ROM].

[4] Initial MCNP6 Release Overview MCNP6 Version 1.0, Los Alamos National Laboratory report LA-UR-13-22934.

[5] Shibata K., Iwamoto O., Nakagawa T., Iwamoto N., Ichihara A., Kunieda S., Chiba S., Furutaka K., Otuka N., Ohsawa T., Murata T., Matsunobu H., Zukeran A., Kamada S., and Katakura J.: "JENDL-4.0: A New Library for Nuclear Science and Engineering," J. Nucl. Sci. Technol. 48(1), 1-30 (2011).

[6] Gunji S., Clavel J.B., Tonoike K., Duhamel I. DESIGN METHODOLOGY FOR FUEL DEBRIS EXPERIMENT IN THE NEW STACY FACILITY. Proceedings of ICNC2019; 2019 Sep. 14-20; Paris, France. [Published online].

[7] PROMETHEE [Internet], France: Institut de Radioprotection et de Sûreté Nucléaire (IRSN); Available from: http://promethee.irsn.org/

[8] Richet Y., Caplin G., Crevel J., Ginsbourger D., Picheny V. Using the Efficient Global Optimization Algorithm to Assist Nuclear Criticality Safety Assessment. Nuclear Science and Engineering. 2013; 175(1):1-18.

[9] SCALE Code System, ORNL/TM-2005/39, Version 6.2.1 (August 2016).

Figure captions

Figure 1. Model of the application case for the sensitivity analysis.

Figure 2. Energy profiles k_{eff} sensitivities to the capture cross sections of ^{28}Si, ^{39}K, ^{40}Ca and ^{56}Fe for CVF = 20 and CVF = 60.

Figure 3. Overview of the two-zones core configurations for the optimization process.

Figure 4. Results of the optimization.

Figure 5. Example of the reshaping work.

Figure 6. Overviews of the optimization core configurations.

Figure 7. Neutron flux densities in different position of the experimental zone.

Figure 8. Sensitivities and reactivity worth depending on of the number of samples.

Figure 9. Overviews of the final core configurations for the STACY experiments.

Table 1. Specifications of new STACY.

Maximum number of fuel rods loading	≤ 900
Fuel composition	UO_2: authorization for an enriched $^{235}U < 10$ wt.% (available fuel enrichment $^{235}U \sim 5$ wt.%)
Effective water height	40−140 cm
Temperature of water moderator	≤ 70ºC
Thermal power	≤ 200 W
Material of cladding	Zircaloy
Effective fuel height (stack height of UO_2 pellets)	142 cm
Diameter of UO_2 fuel pellet	0.82 cm
Outer diameter of cladding	0.95 cm

Table 2. Atomic number densities of the concrete (atoms/barn·cm) [2].

H	$1.374 \cdot 10^{-2}$	^{24}Mg	$9.786 \cdot 10^{-5}$	Na	$9.640 \cdot 10^{-4}$	^{40}Ca	$1.457 \cdot 10^{-3}$
O	$4.592 \cdot 10^{-2}$	^{25}Mg	$1.239 \cdot 10^{-5}$	Al	$1.741 \cdot 10^{-3}$	^{42}Ca	$9.722 \cdot 10^{-6}$
C	$1.153 \cdot 10^{-4}$	^{26}Mg	$1.364 \cdot 10^{-5}$	^{54}Fe	$2.001 \cdot 10^{-5}$	^{43}Ca	$2.029 \cdot 10^{-6}$
^{39}K	$4.295 \cdot 10^{-4}$	^{28}Si	$1.533 \cdot 10^{-2}$	^{56}Fe	$3.165 \cdot 10^{-4}$	^{44}Ca	$3.134 \cdot 10^{-5}$
^{40}K	$5.388 \cdot 10^{-8}$	^{29}Si	$7.761 \cdot 10^{-4}$	^{57}Fe	$7.592 \cdot 10^{-6}$	^{46}Ca	$6.010 \cdot 10^{-8}$
^{41}K	$3.100 \cdot 10^{-5}$	^{30}Si	$5.152 \cdot 10^{-4}$	^{58}Fe	$9.662 \cdot 10^{-7}$	^{48}Ca	$2.810 \cdot 10^{-6}$

Table 3. Major reaction contributions to the k_{eff} sensitivity

CVF = 0.2 (Concrete 20 %)		CVF = 0.6 (Concrete 60 %)	
Critical Radius	21.50 cm	Critical Radius	22.15 cm
^{28}Si elastic	$2.721 \cdot 10^{-3}$	^{28}Si elastic	$7.310 \cdot 10^{-3}$
^{28}Si capture	$-7.656 \cdot 10^{-4}$	^{28}Si capture	$-4.205 \cdot 10^{-3}$
^{28}Si inelastic	$6.264 \cdot 10^{-4}$	^{28}Si inelastic	$2.209 \cdot 10^{-3}$
^{40}Ca capture	$-2.933 \cdot 10^{-4}$	^{39}K capture	$-1.526 \cdot 10^{-3}$
^{39}K capture	$-2.820 \cdot 10^{-4}$	^{40}Ca capture	$-1.319 \cdot 10^{-3}$
^{30}Si elastic	$2.667 \cdot 10^{-4}$	^{56}Fe capture	$-1.262 \cdot 10^{-3}$
^{23}Na elastic	$-2.299 \cdot 10^{-4}$	^{23}Na capture	$-7.992 \cdot 10^{-4}$
^{56}Fe capture	$-2.150 \cdot 10^{-4}$	^{23}Na elastic	$6.907 \cdot 10^{-4}$

Table 4. New STACY Constraints on this optimization work.

Constraint	Value	Constraint type
Number of fuel pins	< 400	Facility constraints and Permission limit
Moderation ratio (V_m/V_f)	0.9−11.0 (core averaged)	Permission limit
Concrete volume fraction	0.00−0.35, 1.00	Facility constraints
Critical moderator water height	40−140 cm, 110−140 cm	Permission limit Experimental limit
(Void) Replacement worth (Δk_{eff})	±10−500 pcm	Experimental limit

Table 5. Parameters, target, and constraint used by the optimization algorithm.

Optimization constraint	Effective multiplication factor (k_{eff})	1 < (achieve criticality)
Optimization target	Integral sensitivity of ^{28}Si capture reaction (S_^{28}Si)	Maximum absolute value
Optimization parameters	P1 (Pitch of the experimental zone) [cm]	1.00–2.55
	D1 (Size of the experimental zone) [cm]	2.55–25.00
	P2 (Pitch of the driver zone) [cm]	1.09–3.00
	D2 (Size of the driver zone) [cm]	15.0–62.0
	w (ratio of the concrete rods in the experimental zone)	0.1–0.9

Table 6. Overview of the optimized three core configurations obtained by PROMETHEE.

Case ID	w	Number of sample rods	Size of test zone	P1 [cm]	D1 [cm]	P2 [cm]	D2 [cm]	k_{eff} (σ<0.00072)	^{28}Si capture (S_^{28}Si)
T25	0.90	563	25x25	1.00	25.00	2.41	54.16	1.07684	$-6.84 \cdot 10^{-3}$
T21	0.90	397	21x21	1.15	24.15	2.13	47.66	1.08773	$-5.27 \cdot 10^{-3}$
T15	0.68	154	15x15	1.50	25.00	3.00	55.44	1.02651	$-2.98 \cdot 10^{-3}$

Table 7. Comparison of the normalized sensitivity values.

Case ID	Area (Number of samples)	^{28}Si Capture Sensitivity (S_^{28}Si)			^{40}Ca Capture Sensitivity (S_^{40}Ca)		
		Thermal* (%)	Intermediate* (%)	Fast* (%)	Thermal* (%)	Intermediate* (%)	Fast* (%)
T25	Center (73)	94.4	3.4	2.2	82.9	3.1	14.1
	Middle (189)	94.6	3.2	2.2	83.3	2.9	13.8
	Outer Edge (301)	95.1	2.8	2.1	84.5	2.6	12.9
T21	Center (23)	96.0	2.3	1.7	**86.6**	2.0	11.4
	Middle (129)	95.9	2.3	1.8	86.3	2.2	11.5
	Outer Edge (245)	95.4	2.6	2.0	**85.1**	2.4	12.5
T15	Center (6)	95.4	2.6	2.0	85.2	2.5	12.3
	Middle (47)	95.3	2.6	2.1	85.0	2.4	12.7
	Outer Edge (101)	95.6	2.4	2.0	85.5	2.2	12.3

*Thermal: < 0.625 eV, Intermediate: 0.625 eV−100 keV, Fast: 100 keV <,
the uncertainty of each value is less than 0.7 %.

Table 8. Expected sensitivities and critical water heights for the optimized core configurations.

Case ID	Number of samples	^{28}Si capture sensitivity		^{40}Ca capture sensitivity	
		Integral value	Per sample	Integral value	Per sample
"Ideal"	about 2600*	$-2.2 \cdot 10^{-2}$	$-8.4 \cdot 10^{-6}$	$-5.8 \cdot 10^{-3}$	$-2.2 \cdot 10^{-6}$
T25 (refinement)	544**	$-9.0 \cdot 10^{-3}$	$-1.6 \cdot 10^{-5}$	$-2.4 \cdot 10^{-3}$	$-4.3 \cdot 10^{-6}$
T21 (refinement)	372**	$-7.7 \cdot 10^{-3}$	$-2.1 \cdot 10^{-5}$	$-2.0 \cdot 10^{-3}$	$-5.4 \cdot 10^{-6}$
T15 (refinement)	140**	$-3.2 \cdot 10^{-3}$	$-2.3 \cdot 10^{-5}$	$-8.2 \cdot 10^{-4}$	$-5.9 \cdot 10^{-6}$
Case ID	V_m/V_f	Void Replacement worth (pcm)	Critical Height for Concrete Samples (mm)	Critical Height for Void Tubes (mm)	dk/dH*** (pcm/mm)
T25 (refinement)	0.55	-319	1188	1280	3.4
T21 (refinement)	1.16	-270	1193	1300	2.9
T15 (refinement)	2.92	-258	1128	1205	3.0

* Used pseudo fuel debris samples (The value of CVF was not 1.0)

** Used full concrete samples (CVF = 1)

*** Around 1100−1300 mm with concrete samples

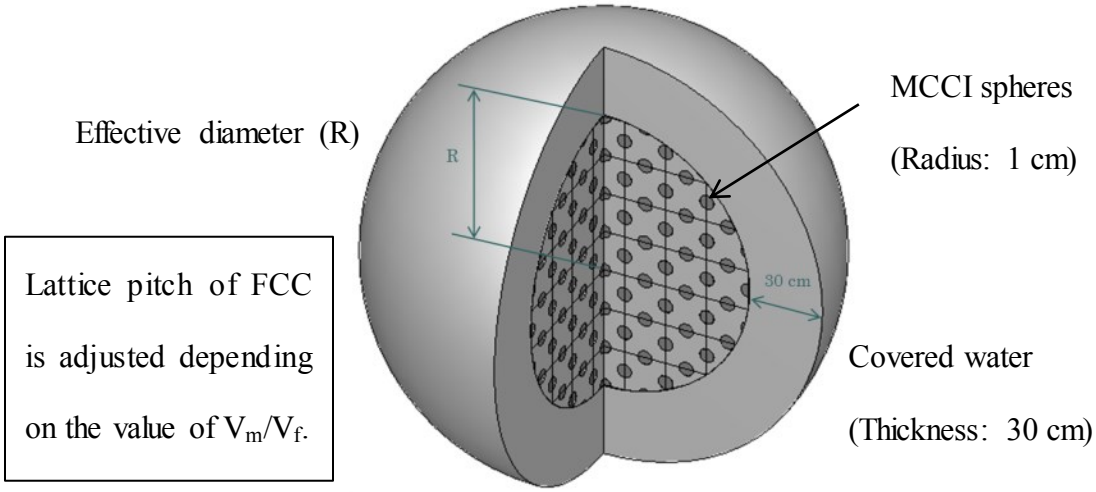

Figure 1. Model of the application case for the sensitivity analysis.

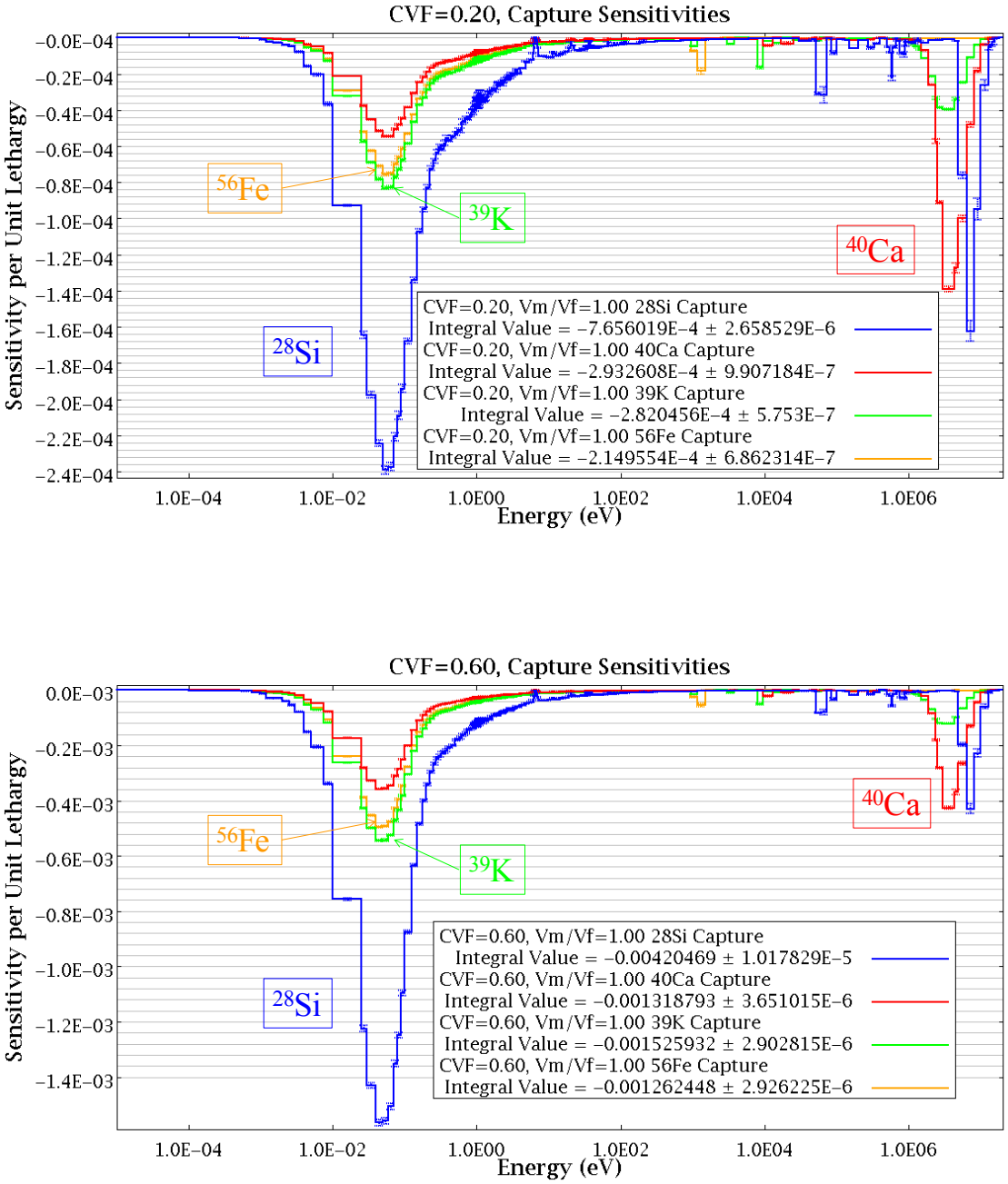

Figure 2. Energy profiles k_{eff} sensitivities [9] to the capture cross sections of ^{28}Si, ^{39}K, ^{40}Ca and ^{56}Fe for CVF = 20 and CVF = 60.

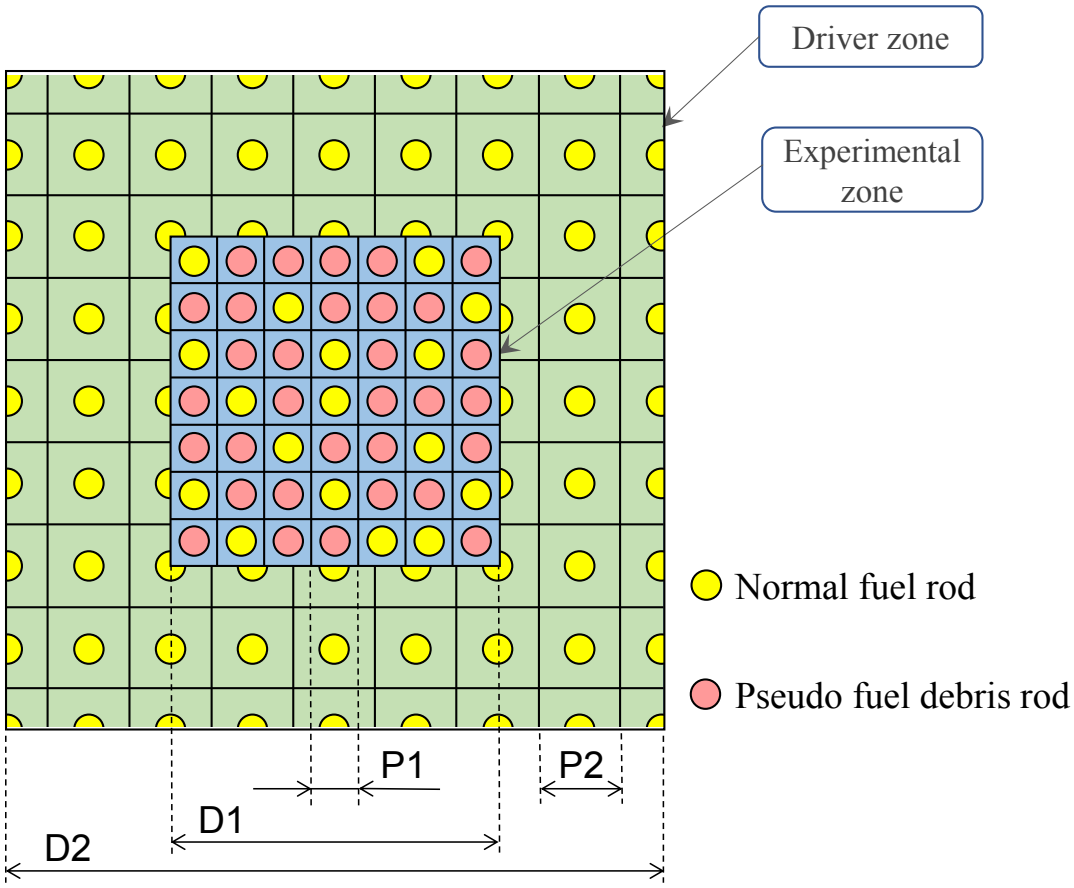

Figure 3. Overview of the two-zones core configurations for the optimization process.

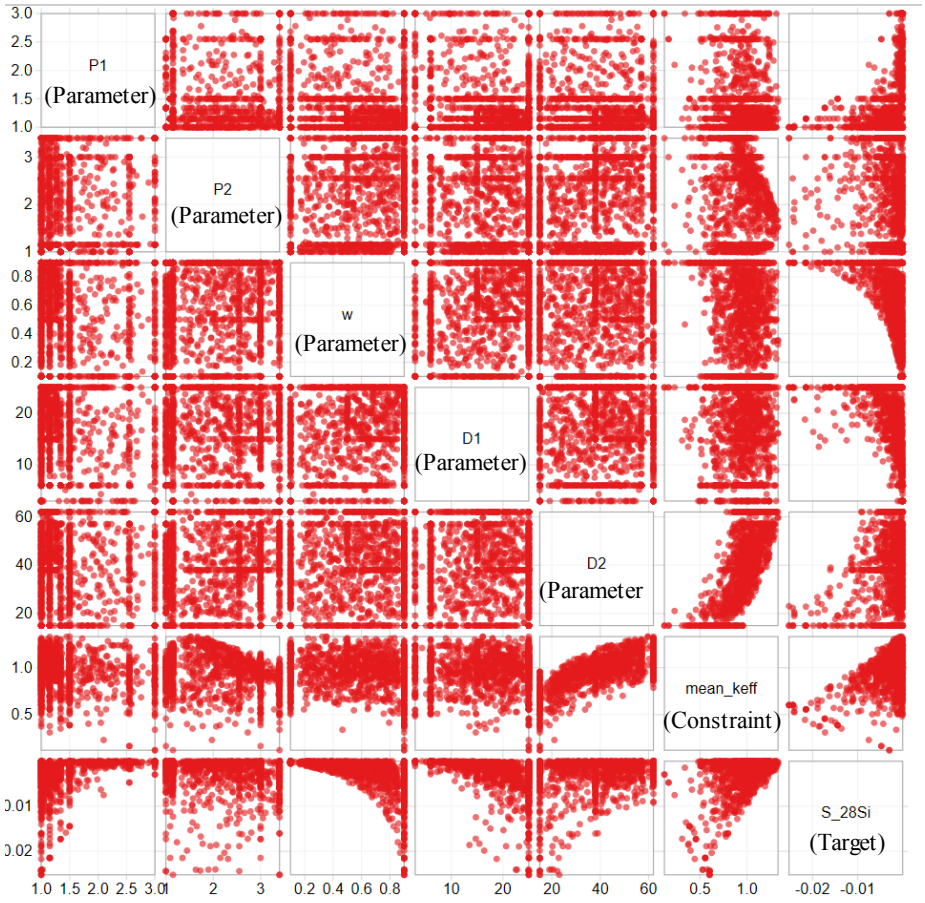

Figure 4. Pairs plot of the optimization results. Each subfigure corresponds to the projection of the calculation points (in red) in function to the parameters or to the target on the same line and column.

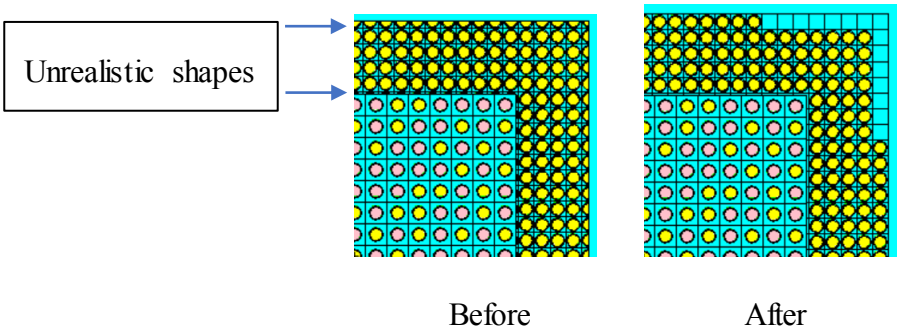

Figure 5. Example of the reshaping work

25x25 Experimental zone

(P1 = 1.00 cm, $V_m/V_f = 0.55$,

563 samples)

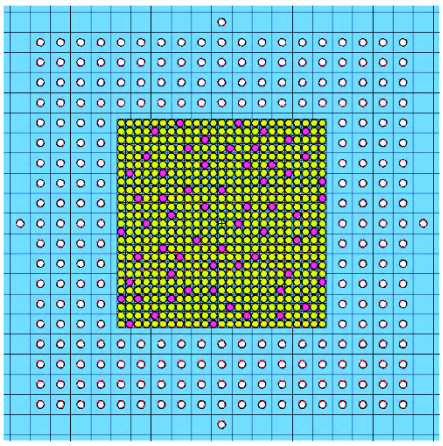

T25

21x21 Experimental zone

(P1 = 1.15 cm, $V_m/V_f = 1.16$,

397 samples)

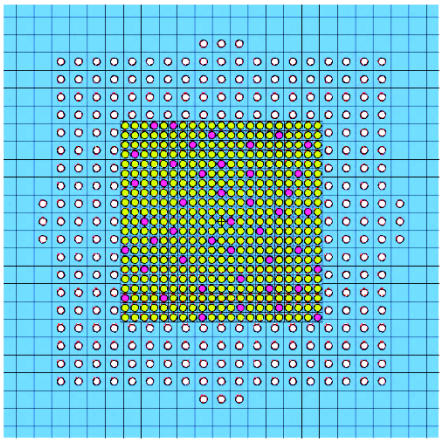

T21

15x15 Experimental zone

(P1 = 1.50 cm, $V_m/V_f = 2.92$,

154 samples)

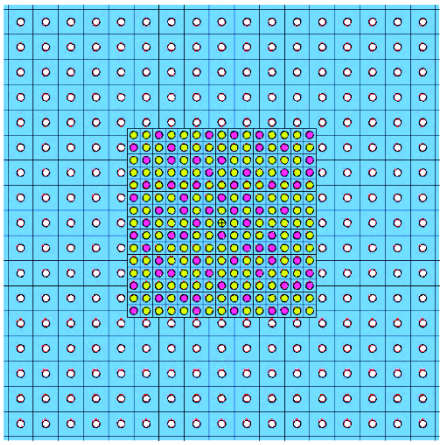

T15

Figure 6. Overviews of the optimized core configurations.

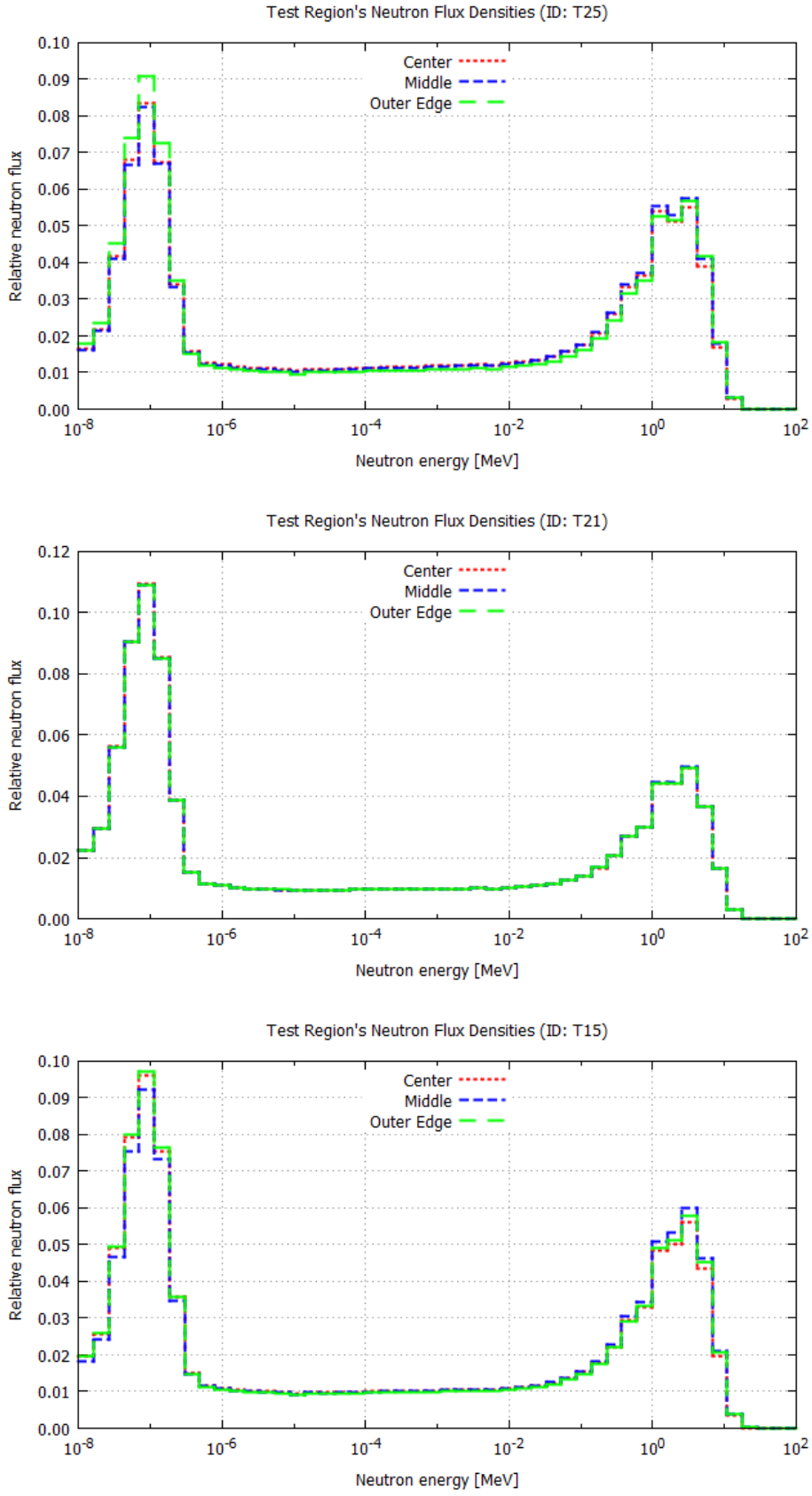

Figure 7. Neutron flux densities in different positions of the experimental zone.

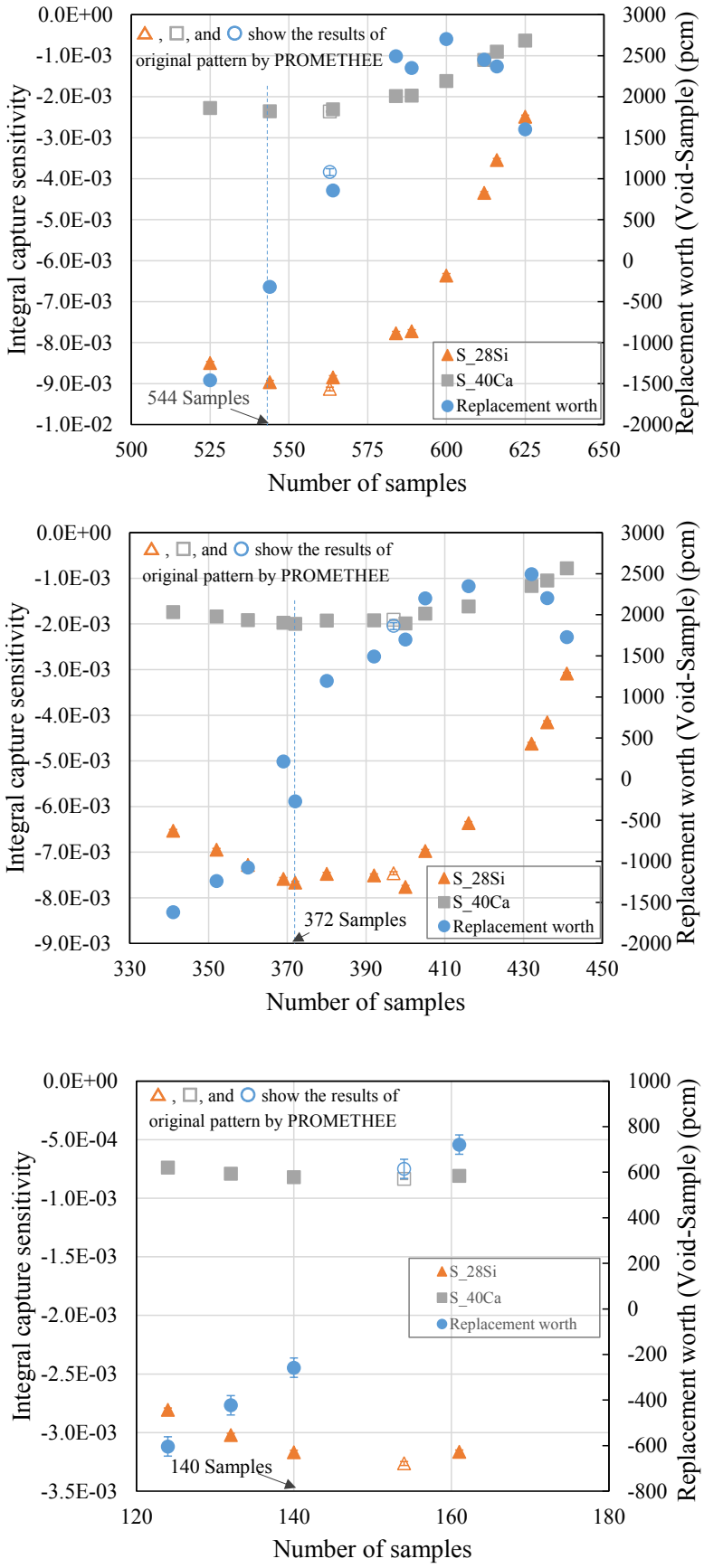

Figure 8. Sensitivities and reactivity worth depending on the number of samples.

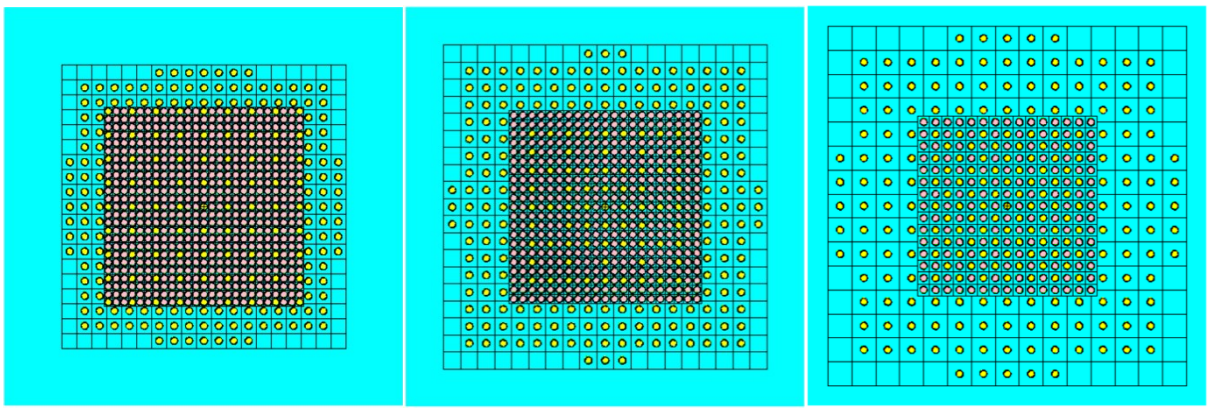

T25 (refinement)	T21 (refinement)	T15 (refinement)
25x25 experimental zone	21x21 experimental zone	15x15 experimental zone
P1 = 1.00 cm	P1 = 1.15 cm	P1 = 1.50 cm
$V_m/V_f = 0.55$	$V_m/V_f = 1.16$	$V_m/V_f = 2.92$
544 samples	372 samples	140 samples

Figure 9. Overviews of the final core configurations for the new STACY experiments.

S. Gunji:

Criticality configuration design methodology apply to the design of fuel debris experiment in new STACY